Coordination of Two High-Affinity Hexamer Peptides to Copper(II) and Palladium(II) Models of the Peptide−Metal Chelation Site on IMAC Resins

Ya Chen,[†] Richard Pasquinelli,[‡] Mohammed Ataai,[‡] Richard R. Koepsel,[§] Richard A. Kortes,[†] and Rex E. Shepherd*[,†]

Center for Biotechnology and Bioengineering, University of Pittsburgh, 300 Technology Drive, Pittsburgh, Pennsylvania 15219, Department of Microbiology/Biochemistry, Dental School of Medicine, University of Pittsburgh, Pittsburgh, Pennsylvania 15261, and Department of Chemistry, University of Pittsburgh, Pittsburgh, Pennsylvania 15260

Received May 13, 1999

The coordination of peptides Ser-Pro-His-His-Gly-Gly (SPHHGG) and $(His)_6$ (HHHHHH) to $[Pd^{II}(mida)(D_2O)]$ ($mida^{2-}$ = *N*-methyliminodiacetate) was studied by ^1H NMR as model reactions for Cu^{II}(iminodiacetate)−immobilized metal affinity chromatography (IMAC) sites. This is the first direct physical description of peptide coordination for IMAC. A three-site coordination is observed which involves the first, third, and fourth residues along the peptide chain. The presence of proline in position 2 of SPHHGG achieves the best molecular mechanics and bonding angles in the coordinated peptide and enhances the interaction of the serine amino nitrogen. Histidine coordination of H_1, H_3, and H_4 of $(His)_6$ and H_3 and H_4 of SPHHGG was detected by ^1H NMR contact shifts and H/D exchange of histidyl protons. The EPR spectra of SPHHGG and HHHHHH attached to the $[Cu^{II}(mida)]$ unit were obtained for additional modeling of IMAC sites. EPR parameters of the parent $[Cu(mida)(H_2O)_2]$ complex are representative: $g_{zz} = 2.31$; $g_{yy} = 2.086$; $g_{xx} = 2.053$; $A_{||} = 161$G; $A_N = 19$G (three line, one N coupling). Increased rhombic distortion is detected relative to the starting aqua complex in the order of [Cu(mida)L] for distortion of HHHHHH > SPHHGG > $(H_2O)_2$. The lowering of symmetry is also seen in the decrease in the N-shf coupling, presumably to the imino nitrogen of $mida^{2-}$ in the order 19 G (H_2O), 16 G (SPHHGG) and 11 G (HHHHHH). Visible spectra of the [Cu(mida)(SPHHGG)] and [Cu(mida)(HHHHHH)] as a function of pH indicate coordination of one histidyl donor at ca. 4.5, two in the range of pH 5−7, and two chelate ring attachments involving the terminal amino donor for SPHHGG or another histidyl donor of HHHHHH in the pH domain of 7−8 in agreement with the $[Pd^{II}(mida)L]$ derivatives which form the two-chelate-ring attachment even at lower pH as shown by the ^1H NMR methods.

Introduction

Immobilized metal ion affinity chromatography (IMAC) is an important method for the separation of proteins having exposed histidine groups.[1−4] One of the most commonly utilized IMAC columns has Cu^{II} sites supported via iminodiacetate (IDA) chelation.[1] IMAC methods are widely used for commercial enzyme purification,[5] in protein separations,[6] and in medical separations of immunoglobins,[7] proteases,[8] human serum proteins,[9] monoclonal IgG antibodies,[10] hepatitus B antibodies,[11] and α-fetoprotein cancer markers.[12]

Attachment of polyhistidine tails ($His_{n=2\ to\ 6}$) fused to a desired peptide or protein has been developed to enhance its affinity to the IMAC column.[13−15] A peptide Ser-Pro-His-His-Gly-Gly (SPHHGG) was recently bioengineered using a phage-displayed library to select for high-affinity binding to of Cu^{II}−IMAC columns.[16,17] SPHHGG has useful properties that allow tagged proteins to be eluted under milder conditions than the $(His)_n$-tagged proteins.[16,17]

The intimate coordination features of how Cu^{II}−IMAC sites bind to proteins or to the affinity tag region has not been studied

[†] Department of Chemistry.
[‡] Center for Biotechnology and Bioengineering.
[§] Dental School of Medicine.

(1) (a) Porath, J.; Carlsson, J.; Olsson, I.; Belfrege, G. *Nature* **1975**, *258*, 598. (b) Porath, J.; Olin, B. *Biochemistry*, **1983**, *22*, 1621. (c) Porath, J. *Trends Anal. Chem.* **1988**, *7*, 254.
(2) Porath, J. *Protein Expression Purif.* **1992**, *3*, 263.
(3) Sukowski, E. *BioEssays* **1987**, *10*, 170. (b) Fatiada, J. A. *CRC Crit. Rev. Anal. Chem.* **1987**, *18*, 1.
(4) (a) Hemdan, E. S.; Zhao, Y. J.; Sulkowski, E.; Porath, J. *Proc. Natl. Acad. Sci. U.S.A.* **1989**, *86*, 1811. (b) Cuirla, S. E.; Peters, E. A.; Barratt, R. W.; Dower, W. J. *Proc. Natl. Acad. Sci. U.S.A.* **1990**, *87*, 6378.
(5) Mrabet, M. T. *Biochemistry* **1992**, *31*, 2690.
(6) (a) Marquez-Mandez, M. *J. Biochem. Biophys. Methods* **1992**, *24*, 51. (b) Sagai, S. L.; Domach, M. M. *Bioseparation* **1995**, *5*, 289. (c) Ehteshanin, G.; Porath, J.; Gusman, R. *J. Mol. Recognit.* **1996**, *9*, 733. (d) Brena, B. M.; Ryden, L. G.; Porath, J. *Biotechnol. Appl. Biochem.* **1994**, *19*, 217.
(7) Boden, V.; Winzerling, J.; Vijayalakshmi, M.; Porath, J. *J. Immunol. Methods* **1995**, *181*, 225.
(8) Winkler, U.; Pickett, T. M.; Hudig, J. *J. Immunol. Methods* **1996**, *191*, 11.
(9) Jiang, W.; Graham, B.; Spicria, L.; Hearn, M. T. *Anal. Biochem.* **1998**, *225*, 47.
(10) Belew, M.; Yip, T. T.; Anderson, L.; Ehrnstrom, R. *Anal. Biochem.* **1987**, *164*, 457.
(11) Canaan-Haden, L.; Ayala, M.; Fernandez-de-Cossio, M. E.; Pedroso, I.; Rodes, L.; Gairlondo, J. V. *Biotechniques* **1995**, *19*, 606.
(12) Andersson, L.; Sulkowski, E.; Porath, J. *Cancer Res.* **1987**, *47*, 3624.
(13) Hochuli, E.; Bannwarth, W.; Dobeli, H.; Gentz, R.; Studer, D. *Bio/Technology* **1988**, *6*, 1321.
(14) Genz, R.; Certa, U.; Takacs, B.; Matile, H.; Dobelj, H.; Pink, P.; Mackay, M.; Bone, N.; Scaife, J. G. *EMBO J.* **1988**, *7*, 225.
(15) (a) Skerra, A. I.; Pfitzinger, I.; Plunkthun, A. *Bio/Technology* **1991**, *9*, 273. (b) Lilius, G.; Persson, M.; Bulow, L.; Mosbach, K. *Eur. J. Biochem.* **1991**, *198*, 499.

10.1021/ic990520z CCC: $19.00
Published on Web 03/02/2000

directly by physical methods. Indirect observations include the following. (1) Histidine side chains must be available.[4,17,18] (2) There is no major assistance by available sulfhydryl or dissulfide linkages.[19] (3) A two-point attachment for peptides to Cu^{II} has been proposed, whereas others claim a single His donor.[20a,b]

In this report the diamagnetic, square-planar [Pd^{II}(mida)] chelate ($mida^{2-}$ = methyliminodiacetate) is used to approximate the distorted tetragonal Cu^{II}−IMAC sites in order to identify which amino acid groups or their side-chain donors of SPHHGG and HHHHHH become attached to the metal site. EPR spectra of [Cu(mida)L], L = SPHHGG and HHHHHH, were also obtained to show additional details of the tetragonal distortion of IMAC sites.

Experimental Section

Preparation of the specialized peptides was carried out as custom syntheses by Quality Controlled Biochemicals (Hopkinton, MA). Their purity was checked by HPLC and by mass spectra. The ^{1}H NMR spectra of SPHHGG and HHHHHH were thoroughly characterized with all assignments as per amino acid residue and sequence.

K[Pd(mida)Cl] was prepared as reported elsewhere,[46] yielding a solid of high ^{1}H NMR purity: a single AB quartet for coordinated glycinato donors with center shifts at 4.37 and 3.41 ppm (J_{ab} = 16.2 Hz) and CH_3 at 2.89 ppm, similar to values of Pd^{II}(iminodiacetate) headgroups.[21] In aqueous solution the Cl^- of the K[Pd(mida)Cl] is labile. $[Cu(mida)]_2$ was prepared as described elsewhere[46] as a light green solid product (fw = 417.4), dimeric as found previously for the $[Cu(ida)]_2$ analogue.[32]

The 300 MHz NMR spectra were obtained on Bruker 300AF spectrometers for samples in D_2O referenced to DSS (0.00 ppm) at 25 °C by following prior procedures for other Pt^{II}, Pd^{II}, and Ru^{II} aminocarboxylate complexes.[22−27]

EPR spectra were obtained at 120 K on a JEOL RE1X EPR instrument with a flowing-nitrogen-cooled cavity. The methods were those of previous publications from this laboratory.[28−31] The spectra were taken on samples of the complexes prepared at ca. 2.5×10^{-3} M in 50:50 water/ethanol solution (pH 6 and 7) and were then frozen inside quartz EPR tubes with liquid nitrogen. The frequency was adjusted to near 9.0 GHz as reported for each spectrum in the figure legends. The modulation amplitude was 5.0 G, and the time constant was 1.0 or 0.3 s depending on the sweep rate of 8.0 or 2.0 min. The center of the field was set to 3000 G, and a 1000 G sweep was made.

UV−visible spectra were recorded on a Varian-Cary 118C spectrophotometer from 800 to 350 nm using quartz 1.00 and 0.100 cm cells. Infrared spectra were recorded on a Perkin-Elmer IR32 instrument on samples prepared as KBr pellets pressed at 9 tons.

Energy-minimized figures showing the atom placement of [Pd^{II}(mida)(SPHHGG)] complex (see the color drawing) were obtained by CHEM-PRO-3D computer software MM2 calculations. A trial structure was generated for [Pd^{II}(mida)(SPHHGG)] according to standard CHEM-PRO-3D drawing procedures. The initial Pd^{II}−N bonds were set initially to literature values for Pd^{II}−amine bonds of 2.02 A.[47] The energy minimization program was utilized to refine the structure, optimizing toward the normal single and double bond lengths, and the standard hybridization angles with adjustments as needed according to electron−electron repulsions between atoms in the structure. Influences of close atom contacts were included in the energy minimization procedure.

An energy-minimized Pd^{II}−N bond length of 1.956 ± 0.013 A was determined on the data set that is deposited in the Supporting Information file. The value of 1.956 Å for the Pd^{II}−N bonds was obtained from three separate initial structure trials. This value was then assigned to the Pd^{II}−N bonds with the in-plane angles initially set to 90.0° and the structure restricted to square−planarity. After minimization, the in-plane angles adjusted to 90.0 ± 0.6°. The MM2 program was executed to minimize the energy of the structure for the square-planar complex including the normal electron−electron repulsions from the lone pairs present on the heteroatoms as required for oxygens and nitrogens in their particular hybridizations. No significant difference in the atom placement was discerned for the three separate trial structures which were brought to final energy minimizations. An examination of all bond lengths and angles revealed that no value exhibits a significant deviation away from standard values that have been deduced for known structures. The data set presented in the drawing of [Pd^{II}(mida)(SPHHGG)] and the representative data in the Supporting Information are both representative of the results obtained from three separate trails.

Results and Discussion

SPHHGG and HHHHHH ^{1}H NMR Spectra. Use of Pd^{II} as an NMR-compatible probe metal ion was recently achieved for Pro-Gly-Ala-His[33] and for several di- and tripeptides.[34] These studies have shown that side-chain coordination of histidyl donors takes preference over peptide nitrogen ionization and amido coordination toward Cu^{II}, Ni^{II}, Pd^{II}, and Pt^{II} that occurs with polyglycine sequences or amino acid polymers lacking coordinating side-chain donors.[35−37] Histidyl units in close proximity take coordination preference and enhance the stability of the metal peptide unit.

The 300 MHz ^{1}H NMR spectra of SPHHGG (Figure 1A) and HHHHHH (available upon request) were assigned at pD 2.12.[38] The following data were obtained by use of separate component amino acid ^{1}H NMR spectra (not shown): (for

(16) Goud, G. N.; Patwardhan, A. V.; Beckman, E. J.; Ataai, M. M.; Koepsel, R. R. *Int. J. Biol. Chromatogr.* **1997**, *3*, 123.
(17) Patwardhan, A. V.; Goud, G. N.; Koepsel, R. R.; Ataai, M. M. *J. Chromatogr.* **1997**, *787*, 91.
(18) Elling, L. *Glycobiology* **1995,** *5*, 201.
(19) Hansen, P.; Anderson, L.; Lindeberg, G. *J. Chromatogr.* **1996**, *723*, 51.
(20) (a) Hansen, P.; Lindeberg, G. *J. Chromatogr.* **1995**, *690*, 155. (b) Todd, R. T.; Johnson, R. D.; Arnold, F. A. *J. Chromatogr.* **1994**, *662*, 13.
(21) (a) Lin, F.-T.; Kortes, R. A.; Shepherd, R. E. *Transition Met. Chem.* **1997**, *22*, 243. (b) Kortes, R. A.; Shepherd, R. E. *Transition Met. Chem.* **1997**, *22*, 68.
(22) Shepherd, R. E.; Zhang, S.; Kortes, R. A.; Maricondi, C. *Inorg. Chim. Acta* **1996**, *244*, 15.
(23) Kortes, R. A.; Shepherd, R. E.; Maricondi, C. *Inorg. Chim. Acta* **1996**, *245*, 149.
(24) Lin, F.-T.; Shepherd, R. E. *Inorg. Chim. Acta* **1998**, *271*, 124.
(25) Chen, Y.; Shepherd, R. E. *Inorg. Chem.* **1998**, *37*, 1249.
(26) Chen, Y.; Lin, F.-T.; Shepherd, R. E. *Inorg. Chem.* **1997**, *36*, 818.
(27) Chen, Y.; Lin, F.-T.; Shepherd, R. E. *Inorg. Chem.* **1998**, *258*, 287.
(28) Shepherd, R. E.; Sweetland, M. A.; Junker, D. *J. Inorg. Biochem.* **1997**, *53*, 1.
(29) Chen, Y.; Sweetland, M. A.; Shepherd, R. E. *Inorg. Chim. Acta* **1997**, *260*, 163.
(30) Zhang, S. S.; Shepherd, R. E. *Inorg. Chem.* **1988**, *27*, 4723.
(31) Johnson, C. R.; Myser, T. K.; Shepherd, R. E. *Inorg. Chem.* **1988**, *27*, 1089.
(32) Dung, N.-H.; Viossat, B.; Busnot, A.; Silicilla-Zarfra, A. G.; Gonzalez-Perez, J. M.; Niclos-Gutierrez, J. *Inorg. Chim. Acta*. **1990**, *169*, 9.
(33) Tsiveriotis, P.; Hadjiliadas, N.; Sovago, I. *J. Chem. Soc., Dalton Trans.* **1997**, 4267.
(34) (a) Tsiveriotis, P.; Hadjiliadas, N.; Stavropoulos, G. *Inorg. Chim. Acta* **1997**, *261*, 83. (b) Rabenstein, D. L.; Isab, A. A.; Shoukry, M. N. *Inorg. Chem.* **1982**, *21*, 3234.
(35) (a) Sigel, H.; Martin, R. B. *Chem. Rev.* **1982**, *82*, 385. (b) Sovago, I. In *Biocoordination Coordination Equilibria in Biologically Active Systems*; Ellis Horwood: Chichester, U.K., **1990**; Chapter 4, p 135.
(36) (a) Margerum, D. W.; Owens, G. D. *Metal Ions in Biological Systems;* Marcel Dekker: New York, 1981; Vol. 12, pp 75−132. (b) Margerum, D. W.; Scheper, W. M.; McDonald, M. R.; Fredericks, F. C.; Wang, L.; Lee, H. D. *Bioinorganic Chemistry of Cooper*; Chapman and Hall: New York, 1993; p 213. (c) Margerum, D. W. *Pure Appl. Chem.* **1983**, *55*, 23. (d) Youngblood, M. P.; Chellappa, K. L.; Bannister, C. E.; Margerum, D. W. *Inorg. Chem.* **1981**, *20*, 1742. (d) Billo, E. J. *Inorg. Nucl. Chem. Lett.* **1974**, *110*, 613.
(37) (a) Cooper, J. C.; Wong, L. F.; Margerum, D. W. *Inorg. Chem.* **1978**, *17*, 261. (b) Kirvan, G. E.; Margerum, D. W. *Inorg. Chem.* **1985**, *24*, 3017.
(38) Spectra were obtained at 25 °C in D_2O with Bruker 300AF NMR's using procedures such as in refs 24−28 or in the following: Chen, Y.; Shepherd, R. E. *Inorg. Chem.* **1988**, *37*, 1249. Chen, Y.; Lin, F.-T.; Shepherd, R. E. *Inorg. Chem.* **1997**, *36*, 818.

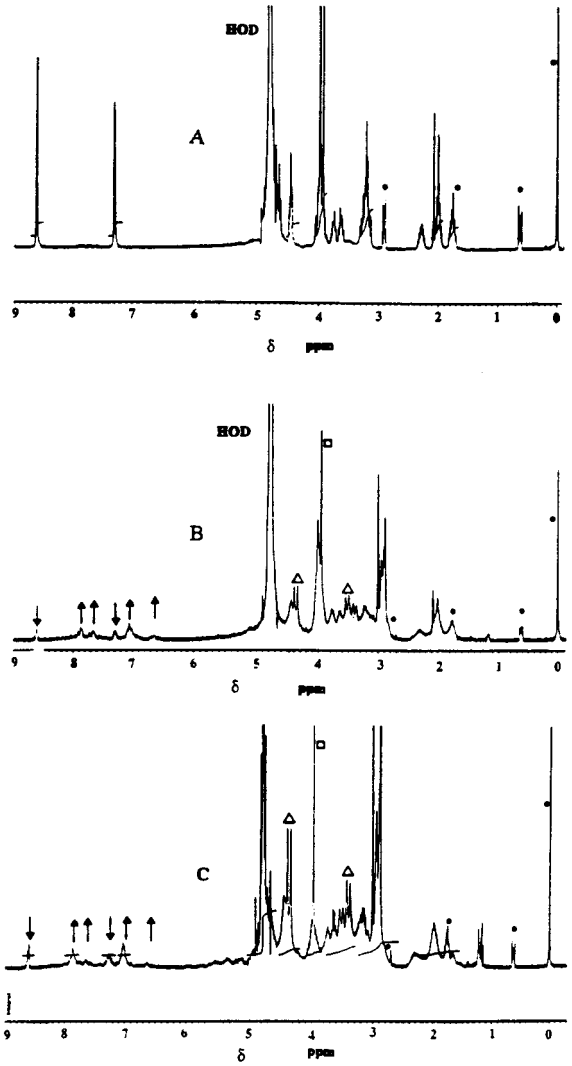

Figure 1. (A) 300 MHz ^{1}H NMR spectrum of SPHHGG in D_2O. Dot markers show locations of DSS reference resonances. See text for other peptide features. (B) 300 MHz ^{1}H NMR spectrum of [Pd^{II}(mida)(D_2O)]/SPHHGG reaction products. Arrows down are for free peptide His features; arrows up are for coordinated His features. Open triangles denote locations of free [Pd(mida)(D_2O)] AB glycinato quartets. Open squares denotes the free rotor glycinato resonance of [Pd(mida)(SPHHGG)]. Dot markers are the DSS reference; see text for other features. (C) 300 MHz ^{1}H NMR spectrum of [Pd(mida)(D_2O)]/SPHH reaction products. Arrows down are for free peptide His features. Arrows up are for coordinated His features. Open triangles, open squares, and dot markers denote the same features as in (B).

SPHHGG) C2H (His) (s) 8.62; C4H (His) (d) 7.30; methine CH (His) (m) 4.66; CH (Pro) (t) 4.44; CH_2 (Gly) 3.99; CH_2OH (Ser) 3.91; CH_2 (Pro) H_a 3.84, H_b 3.62, $J_{ab} = 15$ Hz; CH_2 (His) (m) 3.22; CH_2 (Pro) H_a 2.29, H_b 2.03, $J_{ab} = 6$ Hz; CH_2 (Pro) H_a 1.89, H_b 1.85. For $H_1H_2H_3H_4H_5H_6$, numbered to locate the His positions along the chain, assignments are C2H of the H_2 and H_6 at 8.65, H_3 and H_4 at 8.62, H_1 at 8.71, and H_5 at 8.64; C4H appears at 7.40 for H_1, at 7.31 for H_2 and H_6 as a set, 7.30 for H_5, and 7.26 for H_3 and H_4. The CH (His) resonances appear overlapped at 4.68 ppm for H_2-H_5, at 4.50 for H_1, and 4.30 for H_6; likewise the CH_2's of (His) are at 3.35 ppm for H_1 and 3.15 for H_6, and H_2-H_5 are overlapped at 3.23 ppm.

[Pd(mida)(SPHHGG)] ^{1}H NMR Spectrum. When [Pd(mida)(D_2O)] and SPHHGG are combined at 1:1 stoichiometry in D_2O numerous changes in the shift patterns occur (Figure 1B). All resonances are highly overlapped, and the C2H resonances of the coordinated His donors suffer D/H-catalyzed exchange with time. The H/D exchange weakens the amplitude of these signals but clearly establishes that both histidyl units become bound to Pd^{II}, with resonances shifted magnetically upfield. New features for bound H_3 and H_4 appear at 7.88 and 7.75 ppm for differentiated H_3 and H_4 groups. The CH_2 resonances of the His donors move downfield, being influenced by the charge of the Pd^{II} center but not by direct orbital contact. The glycinato CH_2's of SPHHGG are unaffected, indicative of pendant units. Proline resonances remain unshifted. Histidine CH resonances move downfield slightly and become shoulder features on the HOD resonance. The CH_3 resonance of the [Pd(mida)] fragment moves downfield to 3.08 ppm, indicative of a more positive charge on the Pd−N moiety as required by the displacement of both in-plane glycinato donors of [Pd(mida)] by the coordination of SPHHGG. The glycinato CH_2's of the $mida^{2-}$ ligand appear as a collapsed singlet near 4.00 ppm of freely rotating $-CH_2CO_2-$ groups. The serine CH_2OH resonance remains virtually unchanged. Thus, the ^{1}H NMR data require three binding sites (former positions of the glycinato carboxylates and the in-plane H_2O) in order to account for the differentiated and coordinated H_3 and H_4 donors, the undisturbed P_2 (proline) linkage, the pendant gly-gly portion of the peptide (G_5 and G_6 groups), and the displacement of both $mida^{2-}$ carboxylates. To achieve loss of coordination of the second $mida^{2-}$ glycinato donor requires that the terminal amino donor of serine must displace this group. Approximately 30% of the free SPHHGG and [Pd(mida)(D_2O)] remain after 1.0 h, sufficient time for Pd^{II} peptide equilibria:[34]

$$[Pd^{II}(mida)(D_2O)] + SPHHGG \overset{K}{\rightleftharpoons} [Pd^{II}(mida)(SPHHGG)] \quad (1)$$

A conditional binding constant at pH = 2.34 of 1.45×10^3 ($\log K = 3.16$) is extracted from the initial concentrations.

The energy-minimized atom presentation consistent with the ^{1}H NMR data is shown in the color drawing. The stereochemically active proline appears in the lower right-hand corner with the serine group toward the viewer. The histidines are toward the right side and back of the PdN_4 plane. The calculated $Pd^{II}-N$ bond lengths average 1.956 ± 0.013 A and the in-plane $N-Pd^{II}-N$ angles minimized to $90.0 \pm 0.7°$ by the MM2 procedures that are described in the Experimental Section. All other sp^3 C−C, C−N, and C−O and sp^2 C═N and C═O values were observed to be within accepted variations of standard bond lengths. Calculated angles remain close to those anticipated on the basis of normal hybridizations of the atom centers. No abnormal feature, indicative of severe strain to achieve the forced coordination of the peptide in a way that is not reasonable, was detected in the data sets of three trials that converged to essentially the same atom positions in their energy-minimized structures.

One significant aspect of the coordination mode of the histidyl donors is deserving of comment. The histidine group from the third position along the SPHHGG peptide chain is observed to coordinate in the tautomer with the CH_2 linker to the peptide chain in the remote stereochemistry. This is the "5-tautomer".[46] By contrast, the histidine group from the fourth position along the chain binds to Pd^{II} as the "4-tautomer" with the CH_2 linker to the peptide chain adjacent to the N-3 cordination site. These differences are explained by the steric demand of the peptide chain in having more flexibility with the remote tautomer for the H_3 imidazole, whereas basicity of the coordinating N donor is increased by induction from the CH_2 when it is in the adjacent

Table 1. Selected Energy-Minimized Bond Parameters of [Pd^{II}(mida)(SPHHGG)]

Pd^{II}−N bond	calcd dist (Å)	*N*−Pd^{II}−N angle	calcd angle (deg)
Pd^{II}−N(mida)	1.960	$N(H_3)-Pd^{II}-N(H_4)$	90.7
Pd^{II}−N(ser)	1.936	N(mida)−Pd^{II}−N(ser)	90.4
$Pd^{II}-N(H_3)$	1.951	N(mida)−$Pd^{II}-N(H_4)$	89.3
$Pd^{II}-N(H_4)$	1.977	N(ser)−$Pd^{II}-N(H_3)$	89.5
		N(mida)−$Pd^{II}-N(H_3)$	178.6
		N(ser)−$Pd^{II}-N(H_4)$	174.1

position. Having the imidazole donor of H_4 with the adjacent stereochemistry enables a stronger Pd^{II}−N bond to be created than might be otherwise possible for the last donor that binds the Pd^{II} center to the peptide chain. This donor must hold the coordination strongly to support the remaining G_5 and G_6 linkers to a derivatized protein chain under IMAC conditions. According to the calculations, the advantage of the increased basicity of the H_4 imidazole donor comes at the cost of a very slight increase in bond length to remove steric strain, e.g. 1.977 Å for the $Pd^{II}-H_4$ bond vs 1.951 Å for the H_3 Pd^{II}−N bond.

A complete set of all calculated bond and angle parameters, as well as the numbering system for the 95 atoms in the calculation, are contained in the Supporting Information file. The numbering of the atoms is shown on an energy-minimized structure that is rotated slightly from the view in the color drawing presented here in the text:

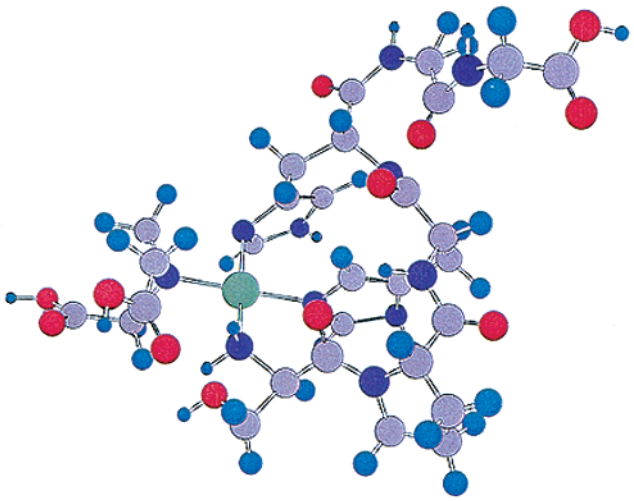

A short list of the key features around the Pd^{II} center is given in Table 1.

[Pd(mida)(HHHHHH)] ^{1}H NMR Spectrum. When HHHHHH is treated with [Pd(mida)(D_2O)] at pH = 2.12, the resultant spectrum at 10.0 min revealed new features showing a loss of free ligand C2H and C4H resonances for H_1, H_3, and H_4 and unchanged features for H_5 and H_6. The addition is complete, as only the displaced glycinato $mida^{2-}$ CH_2's (4.00 ppm) and $mida^{2-}$ CH_3 (3.02 ppm) are observed. The CH resonance of H_2 is little moved. Physical models were constructed to simulate the coordination of $(His)_6$ to [Pd(mida)], adopting the concept that protonation of the terminal amino group would occur in preference to its coordination to Pd^{II}, given the availability of the H_1 histidyl side-chain donor. The best arrangement of the least mechanical strain occurs when H_1, H_3, and H_4 are coordinated, skipping H_2 along the sequence. This is the same position skipped necessarily for SPHHGG, but the models clearly show a steric preference for H_1, H_3, H_4 in preference to H_1, H_2, H_3 or H_1, H_2, H_4, etc. Also, H_1 coordination is clearly indicated by the ^{1}H NMR spectrum.

SPHH and HHGG Tetramer Peptide Data. The conclusions drawn for SPHHGG and HHHHHH coordination were tested at pD = 4.0 with the tetramers SPHH and HHGG without and with [Pd(mida)(D_2O)]. The truncation of the SPHH chain compared to SPHHGG causes a differentiation in the ^{1}H NMR spectrum, particularly for the C4H (His) protons near 7.29 ppm which appear as two sets of doublets, whereas the C2H (His) features are nearly the same at 8.62 ppm. The remaining ^{1}H NMR features of the SPHH ligand are virtually identical to those of SPHHGG except that the CH_2 of serine are a differentiated AB quartet (H_a, 4.03 ppm; H_b, 3.96 ppm, J_{ab} = 18 Hz). Upon addition of 1 equiv of [Pd(mida)(D_2O)] for each resonance of SPHH in the complex, there is a coincident match with the same residues in the SPHHGG complex (see Figure 1C).

These results confirm those of SPHHGG, namely (1) that GG is not needed or involved in coordination, (2) that three sites on Pd^{II} are peptide bound, and (3) that two histidine imidazole groups are coordinated, leaving the need for the terminal amino NH_2 to complete a three-site contact.

The ^{1}H NMR spectrum of HHGG is virtually the same as for HHHHHH, except for the presence of the strong singlet near 4.01 ppm of the free rotor CH_2 resonances of the glycinato linkages. The HHGG pattern actually assists the assignments of the histidine CH_2 and CH groups for H_1 and H_6 of HHHHHH. Likewise, the C2H and C4H patterns for H_1 and H_2 of HHHHHH were assigned on the basis of the patterns for HHGG, since the histidine closest to the protonated terminal amino group will be most downfield.

The addition of 1 equiv of [Pd(mida)(D_2O)] produced a loss of both free ligand histidyl donors of HHGG to coordination. Their new resonances appear differentiated at 8.03 and 7.88 ppm for C2H and at 6.99 for the C4H protons. A weaker group at 7.82 and 6.89 ppm, respectively, hint at a second species of similar environment. The diagnostic 3.99 ppm singlet for the displaced $mida^{2-}$ carboxylates coincide with the CH_2's of the peptide GG functionalities. Both H_1 and H_2 CH_2 protons move downfield as seen in the SPHHGG and HHHHHH cases upon histidyl coordination. The CH_3 of the [Pd(mida)] fragment appears at 3.00, as well as a smaller signal at 2.89 ppm of the unreacted complex.

Upon coordination of all four peptides (SPHHGG, SPHH, HHGG, and HHHHHH) there is evidence for the two required stereochemical isomers of the [Pd(mida)(peptide)] created by the existence of the planar arrangement of the Pd^{II} center and the peptide which establishes a differing environment for the $mida^{2-}$ CH_3 group above or below the plane. Models show that placing the methyl group up relative to the H_3 histidine which adopts a plane perpendicular to the PdN_4 plane will be slightly preferred by fewer repulsions. In each spectum in addition to the major singlet near 3.07 ppm, a smaller singlet appears at ca. 3.03 ppm between the major feature and that of the starting complex at 2.89 ppm. We assign this 3.03 ppm singlet to the less-favored isomer.

The studies of SPHHGG and HHHHHH coordination were repeated at pD = 5.35 and 4.11, respectively. For SPHHGG there is almost the same percentage of free [Pd(mida)(D_2O)] left at equilibrium. For HHHHHH more unreacted [Pd(mida)(D_2O)] appears at pD 4.11, but precipitation removes peptide as well. This shows that chelation is favored at higher pD where coordination of the terminal NH_2 occurs more readily than at pD 2.34 where protons compete with Pd^{II}.

The NMR evidence shows that the hexamer peptides coordinate as S*PH*H*GG and H*HH*H*HH with the tetramer S*PH*H* adopting a three-site attachment to [Pd(mida)]. The

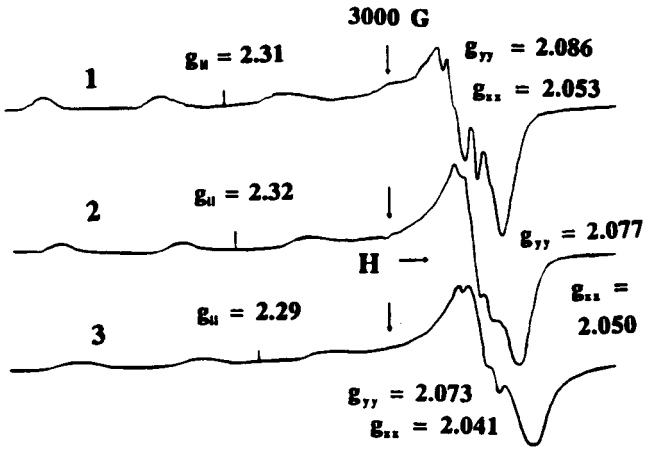

Figure 2. EPR spectra of [Cu^{II}(mida)L] complexes at 120 K in frozen water:ethanol glasses: (1) [Cu^{II}(mida)(H_2O)$_2$] at 20.0 mW power, ν = 9.005 GHz; (2) [Cu^{II}(mida)(SPHHGG)] at 10.0 mW power, ν = 9.060 GHz; (3) [Cu^{II}(mida)(HHHHHH) at 10 mW power, ν = 9.051 GHz; all complexes prepared at 2.5×10^{-3} M with pH ca. 7 before freezing.

tetramer H*H*GG binds only with a two-site contact. Thus, former claims of two-site coordination for Cu^{II}−IMAC column sites may be correct for proteins lacking histidyl side chains near the N-terminus or in rare cases where both positions 1 and 2 are His, followed by noncoordinating groups (Gly, Ala, etc.). Also, the existence of coordinated terminal NH_2 groups is highly pH dependent, favored at high pH (>7) and dissociated at lower values.

The results indicate that the anticipated role of proline in the SPHHGG sequence in gaining affinity at IMAC sites is to provide the best angular arrangement of the peptide donors. Models and the energy-minimized drawing show that H_3 is roughly perpendicular to the $Pd^{II}N_4$ plane and H_4 is at approximately 45° to this plane, producing the least sterically hindered arrangement for the remaining peptide chain. Models of the HHHHHH complex show all three coordinated histidines (H_1, H_3, and H_4) are twisted slightly relative to the $Pd^{II}N_4$ plane in minimizing steric contacts. In principle any amino acid could occupy the second position along the chain, but Pro at position 2 enhances the affinity toward the metal center compared to less rigid and poorer stereochemically orienting groups. The need for high IMAC binding affinity is supplied by the H_3 and H_4 donors. Sterically, the fewest space problems will be obtained when the "linker" portion is Gly-Gly rather than for bulkier groups.

[Cu^{II}(mida)]$_2$ Complex and [Cu^{II}(mida)(H_2O)$_2$] in Solution. The complex "[Cu^{II}(mida)]" was synthesized under pH and concentration conditions that maximize the formation of the monochelate rather than the [Cu(mida)$_2$]$^{2-}$ complex.[39] The complex dissolves into water with loss of the dimeric interaction and will be described in solution with the formulation [Cu(mida)(H_2O)$_2$], consistent with the bis addition of imidazole described later in this text and the isolated [Cu(ida)(im$H$)$_2$]$_2$ complex.[32] The EPR spectrum of [Cu(mida)(H_2O)$_2$], Figure 2-1, correctly differed in its $A_{\parallel}$ value (161 G) from that of [Cu(mida)$_2$]$^{2-}$ (158 G).[40] The frozen solution spectrum of the starting complex was virtually the same as presented by Bonomo et al. for [Cu(ida)(H_2O)] wherein two solution species were detected.[41]

An infrared spectrum of the product shows the presence of two types of coordinated carboxylate donors (υ_{COO} = 1640 and 1600 cm^{-1}) and no protonated carboxylates as speculated previously.[41] Strong features for coordinated water are absent and, thus, consistent with the dimeric bridging by the weaker second interaction of one carboxylate carbonyl for the second Cu center in the dimeric solid. The X-ray structure afforded by the [Cu(ida)(im$H$)$_2$]$_2$ dimer[32] is instructive of the most likely chelation in the [Cu(mida)]$_2$ solid where shared carbonyl donors between Cu^{II} centers occupy imidazole positions in the dimer. It is reasonable that when solvent water molecules are present in the "imidazole" sites that the "axial" glycinato chelate may adopt either a second in-plane coordination or remain axial.

The EPR spectrum of [Cu(mida)(H_2O)$_2$] also gives evidence of two species as shown by broadened, two-humped features in the $g_{\parallel}$ region of the spectrum. The prominent feature is the rhombically-distorted $g_{\perp}$ feature showing separation of the g_{xx} and g_{yy} components near g = 2.06. Specifically for this complex, g_{yy} = 2.086 and g_{xx} = 2.053 whereas $g_{zz} = g_{\parallel}$ = 2.31.

Although N-shf lines often do not appear for sp^3 N donors[42−47] the appearance of N-shf coupling to one N donor is surprisingly strong for the [Cu(mida)(H_2O)$_2$] complex which exhibits a repeating three-line pattern on the g_{yy} component of the $g_{\perp}$ line. A fainter N-shf coupling appears on the g_{xx} component and is overlapped on g_{yy}, making a weaker discontinuity appear on the more major N-shf features of g_{yy}.

Addition of SPHHGG at 1.2 mol of peptide/Cu^{II} complex was accompanied by the visual observation of a darker blue solution, indicative of a greater number of N donors contributing to the ligand field after the addition of the peptide. In the cases of SPHHGG and HHHHHH, coordination of the histidyl donors will take preference in binding the available [Cu(mida)] sites.[33,34] A useful model of the spectroscopic changes caused by alterations of the ligand field of the [Cu(mida)] center by SPHHGG would be the effects produced by the addition of imidazole. On a separate sample of [Cu(mida)(H_2O)$_2$] the d−d electronic transition maximum shifted from 725 nm of the starting complex to 672 nm, appearing darker blue upon addition of 1 equiv of imidazole. Addition of a second 1 equiv of imidazole produced a second change to 662 nm for the d−d maximum. No further spectral change occurred upon adding a third imidazole equivalent. These changes are in agreement with the addition of only two monodentate imidazole donors making [Cu(mida)(im$H$)$_2$] as the solution analogue of the solid-state [Cu(ida)(im$H$)$_2$]$_2$.[32] It is also apparent the mida^{2-} ligand is not displaced by addition of modest excess amounts of imidazole as it is known that [Cu(im$H$)$_n$]$^{2+}$ (n = 4, 5) complexes absorbs at below an upper limit of 620 nm,[42] added evidence that the darker blue sample upon addition of SPHHGG contains the mixed chelation of both components of the mida^{2-} and of the SPHHGG peptide.

[Cu(mida)(SPHHGG)] Visible Spectrum with pH. [Cu(mida)(H_2O)$_2$] was combined with the SPHHGG peptide in aqueous solution at 7.06×10^{-3} M, and the electronic spectrum

(39) Angelici, R. J.; Leach, B. E. *J. Am. Chem. Soc.* **1967**, *89*, 4605.
(40) Molochinkov, L. S.; Radionov, B. K. *Russ. J. Phys. Chem. (Engl. Transl.* **1992**, *66*, 1346.
(41) Bonomo, R. P.; Cali, R.; Riggi, F.; Rizzarelli, E.; Sammartano, S.; Siracusa, G. *Inorg. Chem.* **1979**, *18*, 3417.
(42) Siddiqui, S.; Shepherd, R. E. *Inorg. Chem.* **1986**, *25*, 3869.
(43) Parmley, S. F.; Smith, G. P. *Gene* **1988**, *73*, 305.
(44) Gazo, J.; Bersuker, I. B.; Garay, J.; Kabesova, M.; Kohout, J.; Langfelderova, H.; Melnick, M.; Serator, M.; Valach, F. *Coord. Chem. Rev.* **1976**, *19*, 253.
(45) Hathaway, B. J.; Billing, D. E. *Coord. Chem. Rev.* **1970**, *5*, 143.
(46) Chen, V.; Pasquinelli, R.; Ataai, M.; Koepsel, R. R.; Shepherd, R. E. *J. Inorg. Biochem.* **1999**, *76*, 211.
(47) Barnard, C. F. J.; Russell, M. J. H. In *Comprehensive Coordination Chemistry*; Wilkinson, G. F., Gillard, R. D., McCleverty, J. A., Eds.; Pergamon: New York, 1987; Vol. 5, pp 1114−1116 (Pd^{II}−N (2.02 Å); Pd^{II}−O (1.98 Å)).

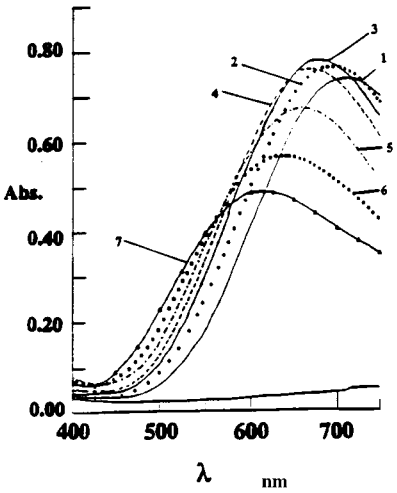

Figure 3. Visible spectra of the 1:1 [Cu(mida)(SPHHGG)] complex as a function of pH with pH values of (1) 3.20, (2) 4.30, (3) 5.35, (4) 6.20, (5) 7.75, (6) 8.85, and (7) 9.45. $[Cu^{II}\ complex]_{tot.} = 7.06 \times 10^{-3}$ M (22 °C).

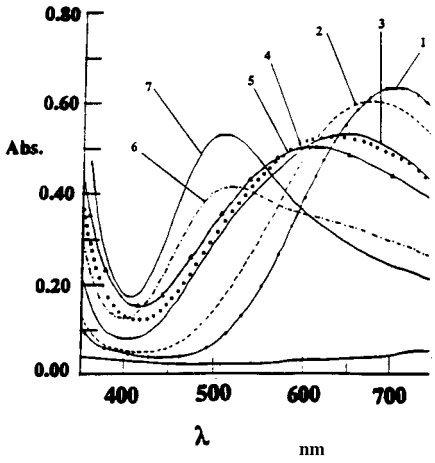

Figure 4. Visible spectra of the 1:1 [Cu(mida)(HHHHHH)] complex as a function of pH with pH values of (1) 2.48, (2) 3.56, (3) 5.28, (4) 6.38, (5) 7.61, (6) 9.34, and (7) 10.76.

of the mixed-ligand complex [Cu(mida)(SPHHGG)] was studied as a function of pH from 3.20 to 9.45. (See Figure 3.) In the pH range of 5.35 the d−d transition shifts to 675 nm, strongly supporting coordination via one histidyl donor as this matches the outcome when one imidazole is bound. As the pH is raised to 6.20 and 7.75 the spectral maximum shifts to 665 nm, and then to 655 nm, similar to when 2 equiv of imidazole coordinate the [Cu(mida)] in-plane sites. A further elevation of the pH to 8.55 gave a shift to 628 nm, like an N_4 in-plane ligand set, including coordination of the terminal NH_2 of serine. This indicates that at higher pH there is a two-chelate ring attachment that cannot be duplicated by three monodentate imidazole donors which lack the stability imposed by chelation.

[Cu(mida)(HHHHHH)] Visible Spectrum with pH. [Cu(mida)$(H_2O)_2$] was also combined with the HHHHHH peptide, each at 7.06×10^{-3} M, and the pH dependence of its coordination was monitored by the changes in its visible spectrum (see Figure 4). At pH 2.48 no coordination of HHHHHH was observed. Increasing the pH to 3.56 caused a shift to a 675 nm maximum, indicative of the binding of one imidazole donor. Higher pH values between 5.28 and 6.38 gave spectral maxima supporting the coordination of two histidine donors out of six. At pH 7.61, a spectrum indicative of four in-plane N donors appears. For these steps to take place, there must be one chelate ring involving presumably an adjacent pair of histidine donors along the chain of HHHHHH. At pH near 7.61 a second chelate ring is established in concert with the increasing number of chelate rings with pH by the SPHHGG peptide. However, here with HHHHHH an additional histidyl imidazole donor is available at a lower pH than is required to deprotonate a terminal amino group. At higher pH appearing at 9.34 and nearly completely at 10.76, there is a switch to a much different coordination environment (510 nm maximum) that appears to the eye as a purple complex. The purple complex is like the peptide-ionized type of coordination well-known for polyglycine and related peptides.[35−37] The spectrum is nearly matched by the combination of [Cu(mida)$(H_2O)_2$] and 1 equiv of triglycine at pH 10.23 ($\lambda_{max} = 535$ nm), but this ligand field is slightly weaker than for HHHHHH, indicating participation of a hystidyl donor as well as two ionized peptide N donors in the [Cu(mida)(HHHHHH)] complex at high pH.[37] The amido-peptide bound species are less important as chromatographically important species, because pH extremes are to be avoided in protein separations.

EPR Spectra of [Cu(mida)(SPHHGG)] and [Cu(mida)(HHHHHH)]. The frozen solution EPR spectrum of [Cu(mida)(SPHHGG)] is given as the second EPR spectrum in Figure 2-2. In the $g_{||}$ region, $g_{||} = 2.32$ and the $A_{||}$ coupling has changed from the starting complex value of 161 G to a new 158 G splitting. The $g_{\perp}$ region has less resolved N-shf features than before with $g_{yy} = 2.077$ and $g_{xx} = 2.050$. It should be noted that the spectrum of [Cu(mida)(SPHHGG)] was not the same as for SPHHGG added to $[Cu(H_2O)_6]^{2+}$, implying retention of the $mida^{3-}$ ligand. Whereas the Pd^{II} complex tends toward strictly square-planar coordination without advantage from coordination of axial ligands, a displaced glycinato arm from an in-plane site on Cu^{II} can still establish a weaker axial ligation, even at an elongated distance. This "extra chelation" that is available to the Cu^{II} center may be important in keeping aggressive chelates such as HHHHHH from simply stripping Cu^{II} from its IMAC sites.

If the two histidine donors of SPHHGG are coordinated, one might anticipate an enhancement in the N-shf signal as long as the geometry at the Cu^{II} center remains close to tetragonal (D_{4h}).[42] This is because the N-shf coupling increases with the percent s character in the bonding MO's, which in turn increase when sp^2 donors including imidazoles are present in the Cu^{II} center's donor set. On the other hand, the N-shf coupling decreases when bond lengthening occurs and with distortion from regular symmetries.[42] On the basis of the evidence that the coordination of SPHHGG to Cu^{II}(mida) occurs through the NH_2 of Ser and two His donors, this must take place by increasing the number of chelate rings that surround the Cu^{II} center. The increased number of N donors, now four instead of the original one in [Cu(mida)$(H_2O)_2$], should occur with elongation of the Cu−N bond to the $mida^{2-}$ sp^3 N donor, as less inductive demand by the Cu^{II} center is present when the Cu^{II} is supplied by other good N donors compared to just one in the starting complex. This is manifest in a decrease in the N-shf coupling constant from $A_N = 19$ G in [Cu(mida)$(H_2O)_2$] complex to $A_N = 16$ G in the SPHHGG adduct (Figure 2-2).

A further decrease is observed when the $(His)_6$ peptide (HHHHHH) is added to the starting complex (Figure 2-3), where $A_N = 11$ G is recorded, and even greater rhombic distortion is observed. For [Cu(mida)(HHHHHH)] EPR parameters are as follows: $g_{||} = 2.29$; $A_{||} = 168$G; $g_{yy} = 2.073$; $g_{xx} = 2.041$.

The loss of distinct N-shf coupling in the cases of the SPHHGG and HHHHHH adducts of [Cu(mida)] is accompanied

by the increase in the rhombic distortion. As an approximate distortion parameter, the g_{yy} and g_{xx} components increase in field separation from ca. 54 G in the starting [Cu(mida)(H_2O)] complex to 65 G for the SPHHGG complex and to 76 G for the HHHHHH complex. This means that the Cu^{II} center "sees" the nearby ligands in a disorted square for the [Cu(mida)(H_2O)$_2$] complex. A more rectangular unit is forced on the Cu^{II} center by chelate ring formation as has been noted previously for the replacement of ammonia donors by ethylenediamine chelate rings, for example.[42] The length of the sides of the ligand field rectangle is further differentiated when the in-plane position that was occupied by a glycinato chelate is displaced by either the serine terminal NH_2 donor for SPHHGG or the first histidine side chain of HHHHHH. The three cases of distortion are shown pictorially here:

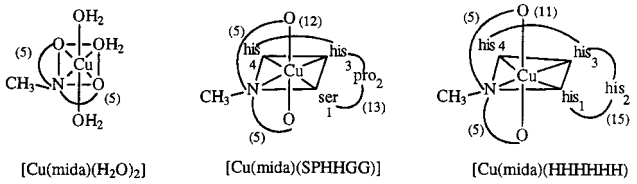

The advantage of proline in the second position of the SPHHGG chain is the physical structure, compactness, and rigidity when SPHHGG is coordinated to [Pd^{II}(mida)], whereas the HHHHHH chain is bulkier and more flexible along the side between the bound first and third histidines. This extra length and flexibility is in concert with the increase in rhombic differentiation in the [Cu(mida)(HHHHHH)] compared to [Cu(mida)(SPHHGG)] EPR spectra. Therefore, the presence of rhombic distortion supports a structure in which the Cu^{II} center of the Cu(mida) fragment establishes two chelate rings with either SPHHGG or with HHHHHH as its second peptide ligand and that a larger chelate ring is present along one side of the rectangular array of "in-plane" donors. A larger difference in "loop size" occurs for HHHHHH with 15 and 11 atom chelate rings compared to 13 and 12 atom chelate rings for SPHHGG as labeled on the drawings above.

Conclusions

These observations support a three-site contact for the protein-separating tags at the Cu^{II}−IMAC columns at pH 7. With larger proteins that lack sufficient numbers of coordinating side-chain donors to make nearby chelate ring attachments to IMAC sites, it may be that a two-point attachment to Cu^{II} must suffice to separate as proposed by Hansen and Lindeberg.[20] And if the species bound by the column retain the same behavior as noted by the visible spectral changes, it is clear that the number of peptide side-chain donors that are attached to the Cu^{II} center varies with pH. Depending on the pH domain which is reported, the SPHHGG and HHHHHH peptides exhibit one donor at low pH < 4, two (or one chelate ring) at pH near 6, and three at pH 7−8. It is highly likely that the high-affinity aspects of the HHHHHH and SPHHGG tags in enhancing the binding of labeled proteins to IMAC columns originates in their ability to a three-point attachment at pH ca. 7 than for a single ring (two-point attachment) from larger proteins.[46]

The [Cu^{II}(mida)(H_2O)$_2$] and [Pd^{II}(mida)(H_2O)] models provide complementary information concerning Cu(IDA)-type IMAC sites. The Pd^{II} model offers superior information concerning exactly which donors along a peptide chain provide the donor atoms for the metal. The d^8 Pd^{II} model cannot mimic properly the flexible adjustment that is based in the d^9 configuration of Cu^{II} which allows for changes in the strength of coordination to the amine donor within the iminodiacetate functionality. This is sensed in only very subtle ways through the EPR evidence of lessened N-shf coupling and rhombic distortion, being greater for HHHHHH than for the SPHHGG adduct. The Cu^{II} center on such site "sees" itself as a more irregular coordination complex. It senses the dimensions of the loops that make up its chelate rings with a peptide tag and considers itself to be less square-planar than the Pd^{II} analogue. In short, it behaves as the "plastic" coordination center[44,45] that is known for traditional coordination complexes of Cu^{II} wherein a wide variation from tetragonal or rhombic (near D_{4h}) to distorted square pyramids and distorted trigonal bipyramids (near C_{2v}) to regular trigonal bipyramids (near D_{3h}) are all common.

Acknowledgment. M.A. expresses appreciation for support of this work from a grant from the Whitaker Foundation. M.A. and R.R.K. acknowledge support from the DOE and NSF. R.E.S. expresses gratitude to the donors of the Petroleum Research Fund, administered by the American Chemical Society, for laboratory support.

Supporting Information Available: Calculated bond parameters for the energy-minimized structure of [Pd(mida)(SPHHGG)] and a structural figure showing the numbering scheme for atoms in the calculation. This material is available free of charge via the Internet at http://pubs.acs.org.

IC990520Z